

Hc2 MEASUREMENTS OF SUPERCONDUCTORS*

J. T. Maniscalco[†], D. Gonnella, D. L. Hall, M. Liepe, and E. Smith
 CLASSE, Cornell University, Ithaca, NY, 14853, USA

Abstract

Recently, Cornell has improved a method for extracting the upper critical field H_{c2} of a thin-film superconductor using four-point resistivity measurements. In the field of superconducting radio-frequency accelerators (SRF), novel materials and processes such as nitrogen-doped niobium and Nb₃Sn may allow for improved SRF performance and cost efficiency over traditional niobium. In this paper we present updated results on H_{c2} measurements for Nb₃Sn, as well as results for niobium prepared with an 800° C bake. We also extract important material properties from these measurements, such as the Ginzburg Landau parameter, the mean free path, and coherence length, which are critical for determining SRF performance.

INTRODUCTION

When considering the utility of alternative materials for use in constructing SRF cavities, several figures of merit exist including the mean free path ℓ , the coherence length ξ , and the Ginzburg-Landau parameter κ which can help gauge the performance of candidate materials against each other. These are related to and can be derived from the upper critical field H_{c2} of the material. Since H_{c2} can only be observed directly at a temperature of 0 K, it must be found through extrapolation. Cornell has developed a method to find H_{c2} of SRF materials, from which the aforementioned parameters can be derived [1]. The method uses a Physical Property Measurement System (PPMS), a device which allows for resistivity measurements at precisely controlled temperatures, magnetic fields, and excitation currents.

APPARATUS AND METHOD

For measurement of SRF materials, a sample up to 1 cm × 1 cm and several millimeters thick is placed on a sample puck (Fig. 1). Four spring-loaded press contacts are applied to the surface, and the assembly is inserted into and sealed inside the cryostat of the PPMS. The four contacts are used in a four-point resistivity configuration.

For a given measurement, the strength of the magnetic field applied by the solenoid and the excitation current for the resistivity measurements are both fixed, and the temperature is swept across the superconducting transition region for the given field and current. We perform resistivity measurements at 0.1 K intervals along the sweep. The result of each

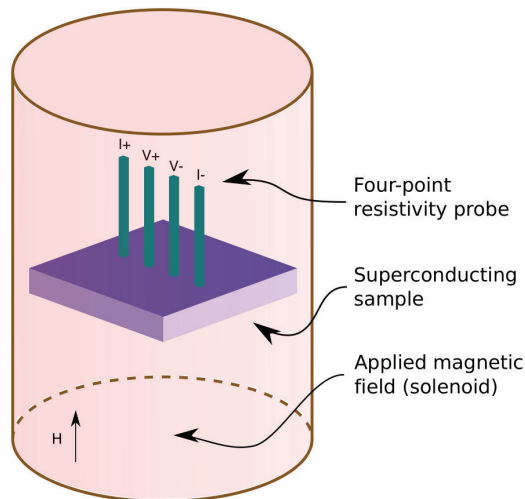


Figure 1: A schematic of a material sample loaded inside the PPMS with four-point resistivity probes attached.

sweep is a characteristic “cliff” graph (Fig. 2). From this, we perform a piecewise linear fit to extract the transition temperature with a 50% resistivity criteria. Uncertainty on $T_c(H, I)$ is taken as the width of the transition region (the steeply ascending central part of the “cliff” shape).

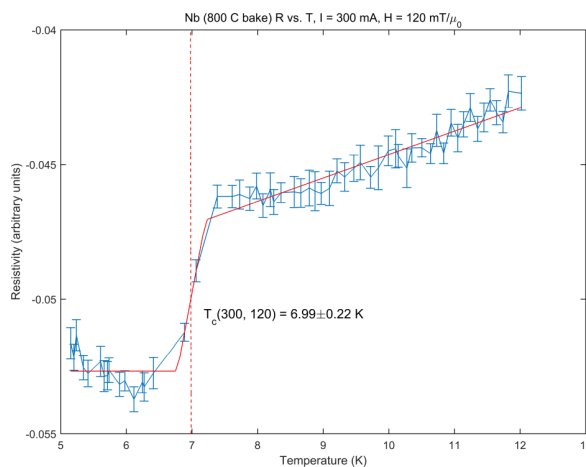


Figure 2: Resistivity measurements at varied temperatures with fixed magnetic field and excitation current. The superconducting transition temperature, $T_c(H, I)$ is chosen with a 50% resistivity criteria.

This temperature sweep is performed at a range of field strengths and excitation currents. Typically, we use the excitation currents 100 mA, 300 mA, and 500 mA. We perform

* This work was supported in part by the NSF grant PHYS-1416318 and by the DOE grant DE-SC0008431. This work made use of the Cornell Center for Materials Research Shared Facilities which are supported through the NSF MRSEC program (DMR-1120296).

[†] jtm288@cornell.edu

a linear fit of T_c at each field strength, extrapolating to find $T_c(H, I = 0)$.

We then perform a least-squares fit of the $T_c(H)$ ordered pairs¹ to extract both $T_c = T_c(0)$ and $H_{c2} = H_{c2}(0)$ for the material according to the empirically derived equation

$$T_c(H) = T_c(0) \left(1 - \frac{H}{H_{c2}}\right)^{\frac{1}{x}} \quad (1)$$

We can also equivalently isolate H_{c2} to find

$$H_{c2} = H \left(1 - \left(\frac{T_c(H)}{T_c(0)}\right)^x\right)^{-1} \quad (2)$$

In previous versions of this work, the variable x was fixed to 2 [1]. Here, to optimize x , we perform the fit according to Eq. 1 while varying x between 0 and 6. We perform a reduced χ^2 analysis at each x and select the x which yields the minimum χ_{red}^2 . For the confidence interval we allow the range of x which yields an increase in χ_{red}^2 less than 10% of the minimum value. This uncertainty is propagated through in combination with the uncertainty from the transition temperatures to give the uncertainty on H_{c2} and on the derived parameters ξ , ℓ , and κ .

We calculate these parameters with the following equations [2–4]:

$$H_{c2} = \frac{\Phi_0}{2\pi\xi^2} \quad (3)$$

$$\xi = 0.739 \left[\xi_0^{-2} + \frac{0.882}{\xi_0 \ell} \right]^{-1/2} \quad (4)$$

$$\kappa = \frac{\lambda_L}{\xi} \sqrt{1 + \frac{\xi_0}{\ell}} \quad (5)$$

See [1] for more information on these derivations.

EXPERIMENTAL RESULTS

In conjunction with other SRF studies at Cornell, we have recently used this method to study two samples: one of Nb₃Sn which had received an EP treatment before coating and one of niobium which received BCP followed by an 800° C bake. Figure 3 show the H vs. $T_c(H)$ data and the H_{c2} fit for the niobium sample, and Fig. 4 shows the goodness-of-fit χ_{red}^2 as a function of fit exponent x , as well as the corresponding H_{c2} and T_c as calculated from the fit at each x . Figures 5 and 6 respectively show the same for the sample of Nb₃Sn. Table 1 shows the extracted parameters for these fits.

For the sample of niobium, the best fit was found with an exponent of $x = 2.1 \pm 0.6$. This exponent is in agreement

¹ One may think of these points as either $T_c(H)$ or $H_{c2}(T)$.

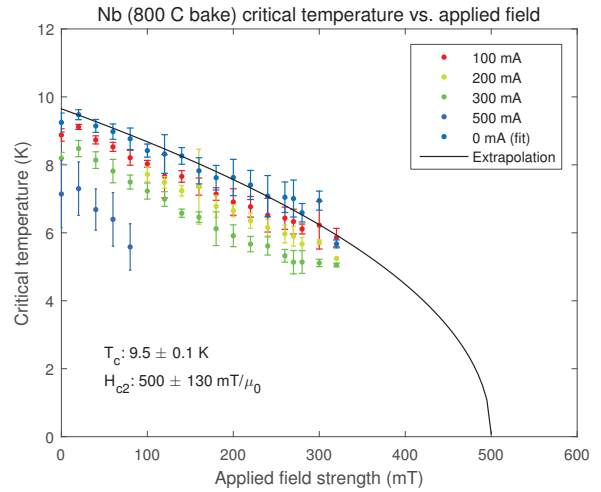


Figure 3: Experimental data and H_{c2} fit for a sample of niobium. Uncertainty written here for T_c and H_{c2} only reflects uncertainty with fit exponent x fixed. For uncertainty values that account for floating exponent, refer to Table 1.

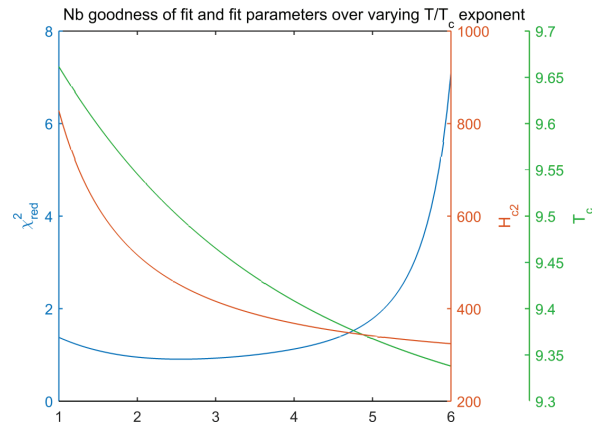


Figure 4: Goodness-of-fit data for the H_{c2} fit for a niobium sample over varying fit exponent x , as well as the corresponding critical temperature T_c and H_{c2} at each exponent.

within uncertainty with the more traditionally used 2 [5]. The upper critical field H_{c2} was found to be 0.50 ± 13 mT, and the critical temperature T_c was found to be 9.5 ± 0.1 K. From this H_{c2} we calculated $\ell = 170 \pm 60$ nm, $\xi = 25.7 \pm 3.3$ nm, and $\kappa = 1.7 \pm 0.5$. Uncertainty in all measurements was dominated by the uncertainty in the fit exponent.

For the Nb₃Sn sample, the exponent yielding the lowest χ_{red}^2 was actually 0.51, with a wide confidence interval of (0,1.30). This fit corresponds to an H_{c2} of 56 T with a confidence interval bounded on the low side by 22 T and unbounded on the high side. The corresponding Ginzburg-Landau parameter κ is 82, with a lower bound of 32 and similarly unbounded on the upper side. The mean free path ℓ was calculated to be 1.7 nm with a confidence interval of (0, 8.7) nm, and the coherence length ξ was calculated to be 2.4 ± 2.4 nm.

This exponent is not in agreement with the traditional value. Moreover, the confidence intervals for the exponent

Table 1: Fit Parameters and Extracted Parameters for Nb and Nb₃Sn Samples

Sample	H_{c2} (T)	T_c (K)	fit exponent x	ℓ (nm)	ξ (nm)	κ
008 (Nb ₃ Sn)	56 (-34, +∞)	18.05 ± 0.02	0.51 (-0.51, +0.79)	1.7 (-1.7, + 6.1)	2.4 ± 2.4	82 (-50, +∞)
017 (Nb)	0.500 ± 0.130	9.5 ± 0.1	2.1 ± 0.6	170 ± 60	25.7 ± 3.3	1.7 ± 0.5

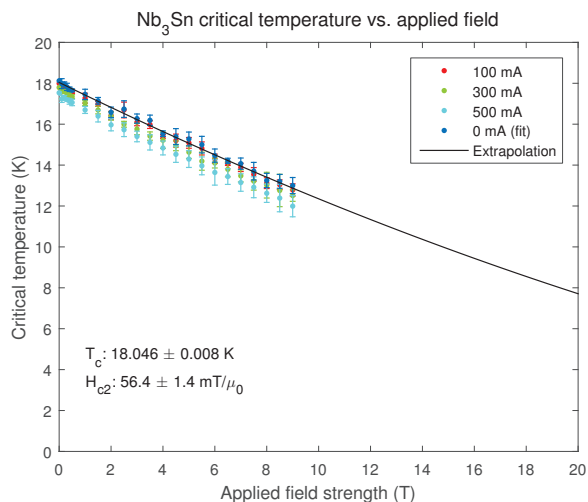


Figure 5: Experimental data and H_{c2} fit for a sample of Nb₃Sn. Uncertainty written here for T_c and H_{c2} only reflects uncertainty with fit exponent x fixed. For uncertainty values that account for floating exponent, refer to Table 1.

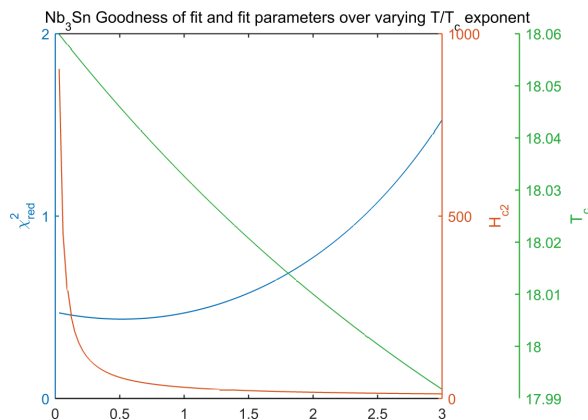


Figure 6: Goodness-of-fit data for the H_{c2} fit for an Nb₃Sn sample over varying fit exponent x , as well as the corresponding critical temperature T_c and H_{c2} at each exponent.

and for the derived parameters is very wide due to the mostly linear behavior of the $T_c(H, I = 0)$ data in the region of measured magnetic fields. In the high field region, above 6 T, the $T_c(H)$ data exhibit a less negatively sloped trend than in the low-field region; one possible explanation for this behavior, atypical of $T_c(H)$ diagrams, is that there are multiple phases of Nb₃Sn in the sample, with different properties, including T_c and H_{c2} . This possibility is supported by previous measurements of Nb₃Sn using other methods, including XRD, EDX, and high-power pulsed RF measurements [6].

To investigate this further, it will be critical to probe higher fields with the PPMS. Previously, our measurements had

been limited by a maximum field of 9 T, but a new PPMS has been installed recently at the Cornell Center for Materials Research (CCMR) which supports fields up to 14 T; future measurements will use this new machine.

Looking forward, iterations of this work will focus on understanding the variation in fit exponent x , investigating the possibility of multiple phases in the material, and on determining other possible explanations for the unusual behavior of Nb₃Sn.

CONCLUSION

We at Cornell have developed a method to find the upper critical field H_{c2} of type-2 superconductors using a PPMS by measuring $T_c(H, I_{exc})$ at a range of fields and excitation currents, fitting linearly to find $T_c(H, 0)$, and fitting according to Eq. 1 to calculate H_{c2} and T_c . In this work we have allowed the fit exponent x to vary (whereas in previous work we have fixed it to 2), selecting as the best x that which yields the lowest χ_{red}^2 for $T_c(H)$. From H_{c2} we extract ξ , ℓ , and κ .

In this work, we have performed these measurements on two samples, one of Nb and the other of Nb₃Sn. The results of these measurements are shown in Table 1. The results of the Nb₃Sn sample suggest that there may be multiple phases in the material, with distinct parameters. Future measurements are needed at high fields to investigate this possibility.

REFERENCES

- [1] J. T. Maniscalco, D. Gonnella, D. L. Hall, M. Liepe, and S. E. Posen. H_{c2} Measurements of Nb₃Sn and Nitrogen-Doped Niobium using Physical Property Measurement System. In *Proceedings of IPAC 2015*, May 2015.
- [2] M. Tinkham. *Introduction to Superconductivity*. Dover Publications, Inc., 2 edition, 1996.
- [3] T. P. Orlando, E. J. McNiff, S. Foner, and M. R. Beasley. Critical fields, Pauli paramagnetic limiting, and material parameters of Nb₃Sn and V₃Si. *Phys. Rev. B*, 19:4545–4561, May 1979.
- [4] M. Hein. *High-Temperature-Superconductor Thin Films at Microwave Frequencies*. Springer, 1999.
- [5] S. E. Posen. *Understanding and Overcoming Limitation Mechanisms in Nb₃Sn Superconducting RF Cavities*. PhD thesis, Cornell University, 2015.
- [6] D. L. Hall, M. Liepe, J. T. Maniscalco, and S. E. Posen. Recent Studies on the Current Limitations of State-of-the-Art Nb₃Sn Cavities. In *Proceedings of IPAC 2015*, May 2015.